ORIGINAL PAPER

Experimental Evaluation of Three Local Exhaust Ventilation Systems Designed to Reduce Ultrafine Dust Emission During a Polishing Process

Mohamed Nejib Saidi[1] · Abdelhakim Djebara[2] · Victor Songmene[3] · Ali Bahloul[1]

Abstract

Aerosol transport is a fundamental phenomenon in many environmental and industrial applications. The study of the dispersion of aerosols, such as contaminants, in the workplace and the search for solutions to capture them are the biggest challenges currently faced in the field of occupational safety and health. In addition, laws and regulations that limit the level of worker exposure to contaminants in workplaces are becoming stricter. The aim of this study was to help reduce exposure to dust, including crystalline silica dust, emitted during the granite polishing process. During this process, the ultrafine particles generated are more difficult to capture than the fine ones, especially in rotational polishing, which causes the worst cases of dust exposure. An experimental test bench was set up to simulate ultrafine particle dispersion and assess three solutions for reducing worker exposure during the rotational polishing process. The use of the test bench allowed experiments to be performed while avoiding human exposure. Results showed that the test bench efficiently simulated the dispersion of ultrafine particle dust. Three solutions designed to reduce dust emissions, based on local exhaust ventilation, were evaluated on the test bench: a push–pull system, a dust shroud and a tool with integrated suction slots. They proved to be more than 95% effective. The results of this work highlight that the performance of local exhaust ventilation systems is very sensitive to the suction flowrate and the speed of the rotating disc, thus illustrating the complexity of dust removal associated with polishing processes in industrial environments.

Keywords UFPs · Dispersion · Experimental simulation · Dry polishing · LEV systems

1 Introduction

Dust containing quartz is present in many industries, including the construction, cement and ceramic manufacturing, granite and mining industries. A significant number of workers are thus exposed to this dangerous dust. Indeed, several studies have shown a relationship between lung disease, worker mortality and their exposure to quartz dust (Liu et al. 2013; McDonald et al. 2005; Pelucchi et al. 2006; Rushton 2007; Verma et al. 2011). Prolonged exposure of workers to high levels of quartz dust can lead to serious lung diseases such as silicosis and lung cancer (Fanizza et al. 2007; Martínez et al. 2010; Steenland and Ward 2014). Laboratory studies show that quartz ultrafine particles (UFPs) are more dangerous to respiratory cells than fine particles (FPs) and that they have a greater inflammatory effect than FPs (Ahmad et al. 2011; Kusaka et al. 2014). When humans are exposed to UFP dust, a large portion of inhaled UFPs measuring less than 100 nm in diameter are deposited in the alveolar sacs of the lungs (ICRP 1994). Numerical simulation of UFPs deposited on the surface of the lung's inner walls shows that the majority of these UFPs have a diameter of 100 nm or less (Zhang et al. 2005). When deposited in large quantities, these UFPs create sites of interaction that promote their absorption by the human body and can transmit toxic substances to it. Many countries have local rules defining the permissible exposure limits (PELs) not to be

✉ Ali Bahloul
  ali.bahloul@irsst.qc.ca

1 Institut de recherche Robert-Sauvé en santé et en sécurité du travail (IRSST), 505 De Maisonneuve Boulevard West, Montreal, QC H3A 3C2, Canada

2 École Nationale Polytechnique de Constantine (ENPC), BP 75, A, Nouvelle Ville RP, Constantine, Algeria

3 École de Technologie Supérieure (ÉTS), 1100 Notre-Dame Street West, Montreal, QC H3C 1K3, Canada

exceeded when handling hazardous materials such as quartz. In North America, for example, the quartz PEL is 0.1 mg/m^3 in Quebec (Canada) (ROHS 2019) and 0.05 mg/m^3 in the USA (OSHA 2019). Workers in the dry granite manufacturing industry, such as rotational polishing of countertops, are exposed to quartz levels far exceeding the limits (Phillips et al. 2013). In this case, the dust particles released during dry polishing are the most difficult to control because of their trajectory, which is dictated by the rotational movement of the tool (Goyer et al. 2010).

The polishing process is carried out by several passes of rotating tools with abrasive grains, starting with the largest abrasive grains and ending with the finest (Li et al. 2006; Saidi et al. 2015; Xu et al. 2003; Yavuz et al. 2011). The process can be divided into two parts: the roughing phase at the beginning, characterized by the generation of a large quantity of FP dust; and the finishing phase at the end, characterized by a smaller quantity of FP dust. The quantity of UFP dust generated is inversely proportional to the quantity of FP dust produced during the two phases of granite polishing (Saidi et al. 2015; Xu et al. 2003). The dry rotational and translation-free polishing of granite (where the varied polishing parameter is only the spindle speed and the feed rate is set to zero) is the worst-case scenario to which workers may be exposed (Saidi et al. 2018). Indeed, in this case, the back-and-forth movement generated by the feed rate, which helps to dilute the dust particle concentration and consequently to reduce dust exposure (Yaonan et al. 2014), does not exist. This kind of polishing resembles regular polishing, especially in the emission and dispersion of particle dust. In this polishing process, as in regular granite polishing, a high concentration of FPs and UFPs remains close to the polishing tool. It is therefore necessary to implement a solution for capturing dust particles at the source in order to protect workers from exposure. An experimental test bench and a computational fluid dynamics simulation (CFD) were run in an earlier study based on rotational polishing (Bahloul et al. 2019). Test benches and CFD simulations help to study the polishing process and develop solutions for capturing dust at the source while avoiding human exposure. The results of that study showed that both the experimental test bench (using UFPs of NaCl and CO$_2$ gas tracer) and CFD simulation (using CO$_2$) efficiently simulated the dispersion of UFPs generated in the polishing process for a high spindle speed of 2500 rpm. The study documented here used the same experimental test bench (Bahloul et al. 2019) to assess three LEV systems designed to reduce UFPs generated during the polishing process.

There are commercial solutions recommended reducing workers' exposure to dust during the rotational polishing of granite, solutions such as general ventilation and local exhaust ventilation systems (LEV) (ACGIH 2010). The use of general ventilation is difficult to apply and more expensive to implement, particularly in small and medium-sized enterprises (Goyer et al. 2010). The use of exterior hoods as a LEV system to extract dust is recommended in the case of granite finishing (ACGIH 2010). However, this solution is not very effective in the case of rotational polishing. In this case, the dust particles are emitted with a significant velocity and their trajectory cannot be precisely defined, making their capture difficult (Goyer et al. 2010). The use of a dust shroud as a LEV system on the rotational polishing disc combined with the use of water reduces exposure, but the quartz rate remains higher than the PELs (Akbar-Khanzadeh et al. 2007; Croteau et al. 2002; Johnson et al. 2017; Simcox et al. 1999; Songmene et al. 2018). In addition, the use of water is more efficient in reducing the FPs than the UFPs generated during the granite polishing process (Songmene et al. 2018). There is, therefore, great interest in further research on solutions for capturing dust particles emitted during the rotational polishing process, and in particular, for capturing ultrafine particles.

Removal of ultrafine particles and aerosols, especially during the rotational polishing process, poses a major challenge. To achieve this goal, this investigation was divided into two parts. The first part sought to validate the efficiency of the experimental test bench (using UFPs of NaCl) in simulating UFP dispersion during the rotational polishing process. The second part studied the efficiency of three LEV systems (push–pull system, dust shroud and tool with integrated suction slots) in capturing dust emissions during this process. The use of the test bench-made experiments possible without human exposure.

2 Materials and Methods

2.1 Experimental Design and Conditions

The test bench shown in Fig. 1 was designed to simulate UFP dispersion in the rotational polishing process. It was installed in a containment pen with a volume of $3 \times 3 \times 2.6$ m^3 to prevent external contamination and drafts due to room ventilation. The test bench consisted of a mini-milling machine 2000 (Sherline Products, California, USA) with a spindle speed (V_s) varying from 70 to 2800 rpm. A rotating disc, 5 inches in diameter, was mounted on the spindle of the machine and positioned parallel to the surface of the table. An injection plate providing a uniform UFP supply was installed under the disc at a distance of 0.5 mm. 42 holes of 3 mm-diameter are used for the UFP injection. To avoid oxidation of the table by salt (NaCl), the connection between the table and the injection plate was made of Plexiglas. UFP are ejected by the rotational motion of the disc to simulate UFP dust dispersion during the polishing process. The dust particles generated by granite polishing are spherical and

Fig. 1 3D drawing of the experimental device
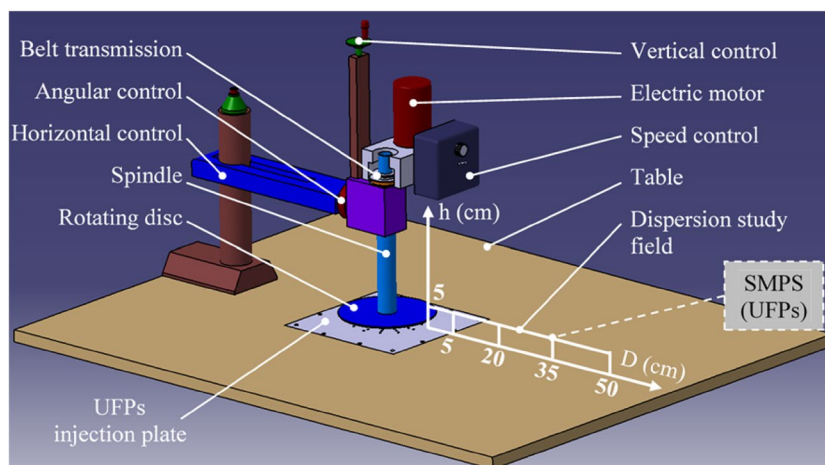
cubic in shape (Saidi et al. 2018). In this study, NaCl particles were used as tracer particles to study particle dispersion. These particles have both cubic and spherical shapes (Silverman and Billings 1956). The use of NaCl ultrafine particles was, therefore, deemed appropriate for simulating granite particle dispersion. Figure 2 shows the supply chain of UFPs used in this investigation. The aqueous salt solution was transformed by a 6-jet atomizer 9306A (TSI Inc., Minnesota, USA) into aerosols. The aerosols were passed through a tube filled with silica gel to remove their humidity. The dried UFPs obtained were then passed through a flowrate regulator. UFPs were injected under the rotating disc at the desired flowrate.

UFP dispersion in horizontal direction D was measured at four checkpoints located at a fixed vertical distance h of 5 cm (see the dispersion study field in Fig. 1) and compared to their dispersion in the polishing process. A spectrometer Scanning Mobility Particle Sizer (SMPS) $(3080 + 3085 + 3775)$ (TSI Inc., Minnesota, USA) was used to measure the UFP concentration. Each measurement took 1 min and was repeated six times. The UFP dispersion

results were compared to those found obtained in the polishing process. The validation of the experimental test bench was performed with a low spindle speed of 1000 rpm. In fact, in earlier work, the experimental test bench had already been validated with a high spindle speed of 2500 rpm (Bahloul et al. 2019).

2.2 Investigated LEV Systems

In this study, three solutions—based on local exhaust ventilation (LEV)—for containing and removing dust emitted by the polishing process were investigated in the test bench. The first solution for UFP capture was the push–pull system shown in Fig. 3. Push–pull systems are usually used to remove contaminants released with practically no velocity into still air, as in the case of open surface tanks (Wang et al. 2016). In the current study, a push–pull system was designed and adapted to capture the particles generated during the polishing process (Fig. 3). It consisted of using blowing air to push the UFPs ejected by the rotating disc to the exhaust hood. To measure the efficiency of this LEV system, the UFP

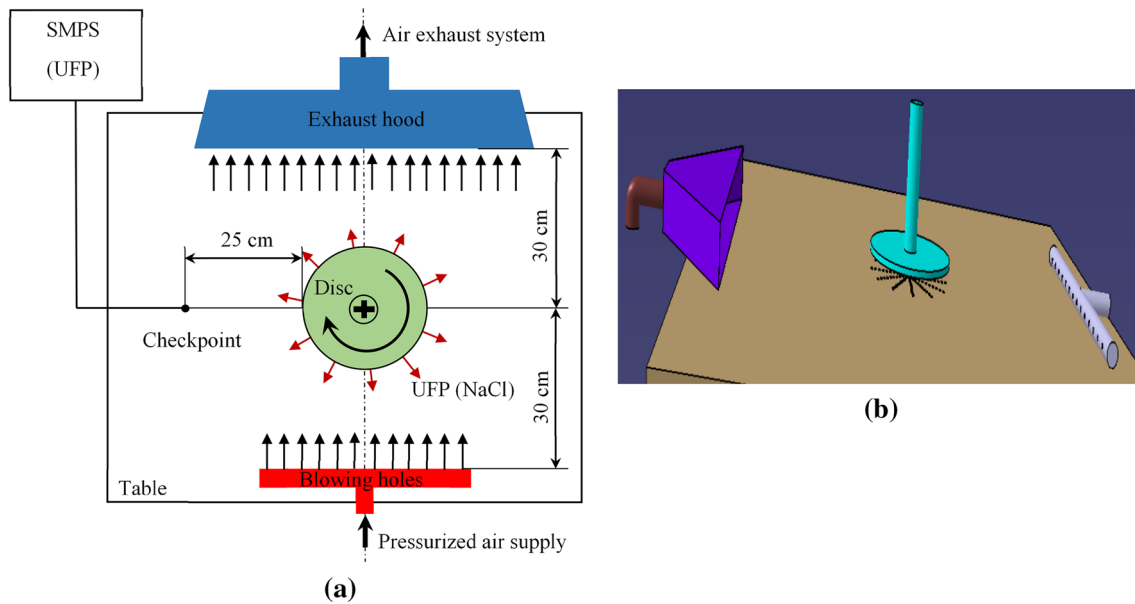**Fig. 2** The supply chain of dry UFPs of NaCl
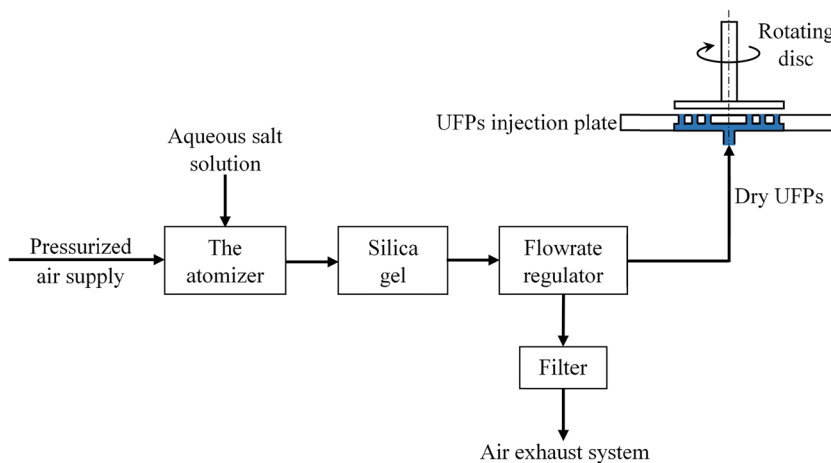
Fig. 3 The push–pull system: **a** set-up **b** 3D drawing

number concentration (CUFP) was measured at a checkpoint 25 cm away from the rotating disc and perpendicular to the blowing airflow (outside of the airflow effect). The suction flowrate of the exhaust hood was changed to 1250, 1750 and 2250 l/min and the blowing flowrate was increased gradually until the desired efficiency was reached. Experiments were performed for spindle speeds of 1000, 1500, 2000 and 2500 rpm. The second solution for UFP capture was the dust shroud system shown in Fig. 4. The dust shroud mounted on the rotating disc allowed dust extraction directly at the source. There was a gap of 1 mm between the dust shroud

and the table. The efficiency checkpoint for this LEV system was located at a distance of 1 cm from the rotating disc. Experiments were performed for spindle speeds of 1000, 1500, 2000 and 2500 rpm. The first and second solutions are well suited for dust capture in the polishing of flat surfaces (as in the polishing of countertops). The third solution for UFP capture was the tool with an integrated suction slot system shown in Fig. 5. This solution involved modifying the design of the rotating disc (the tool) by integrating an internal suction path, which allowed the evacuation of the dust released during polishing. Six suction slots were made in
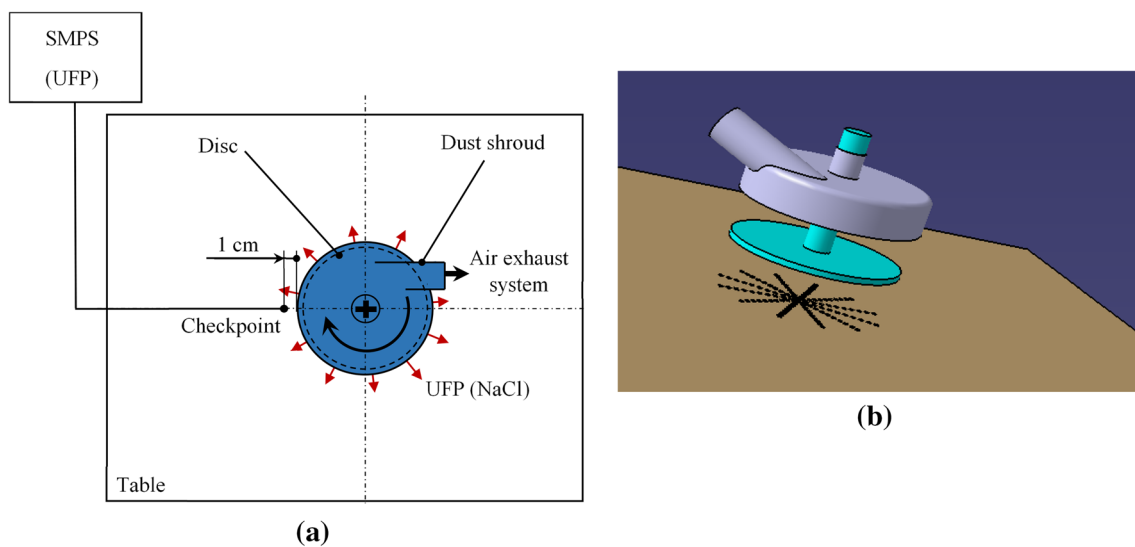

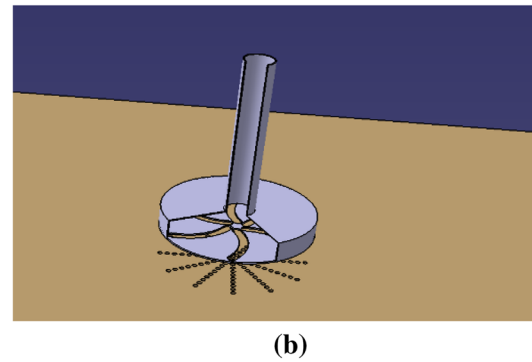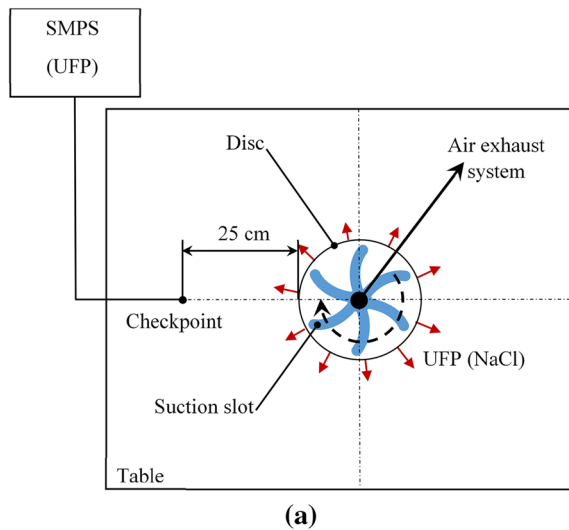**Fig. 4** The dust shroud: **a** set-up **b** 3D drawing

Fig. 5 The tool with integrated suction slots: **a** set-up **b** 3D drawing

the underside of the rotating disc, which would be in contact with the workpiece. This solution allowed the dust particles to be suctioned off at the closest possible point to the disc/workpiece contact. The efficiency checkpoint for this LEV system was located at a distance of 25 cm from the rotating disc. Experiments were performed for spindle speeds of 1500 and 2500 rpm. Efficiency is a well-established indicator in the field of occupational hygiene for evaluating the performance of LEV systems, and is calculated as follows:

$$\text{Efficiency}\,(\%) = \left(1 - \frac{\text{CUFP}_{\text{without LEV system}}}{\text{CUFP}_{\text{with LEV system}}}\right) \times 100. \quad (1)$$

3 Results and Discussion

3.1 Validation of the Simulation Test Bench

This part of the study sought to validate whether the experimental test bench could simulate the dispersion of UFPs generated during the polishing process.

3.1.1 UFP Supply Calibration for the Simulation Test Bench

Figure 6 shows the calibration of the UFP supply flowrate with $V_s = 1000$ rpm and $h = 5$ cm. It shows the UFP dispersion over horizontal distances. For a 0.5 l/min supply flowrate, the CUFP was diluted immediately upon coming out of contact with the rotating disc. For 1 to 4 l/min supply flowrates, the CUFP peaked at a horizontal distance (D) of between 15 and 20 cm (as in the granite
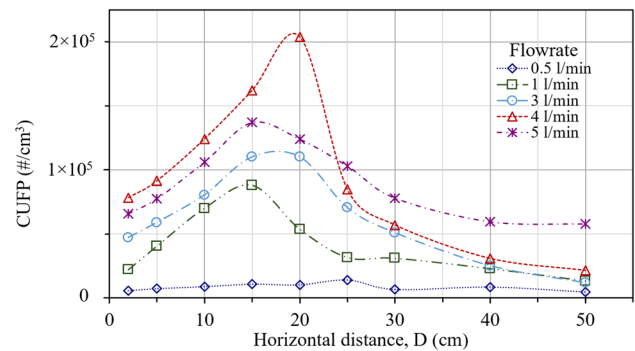

Fig. 6 Calibration of the UFP supply flowrate with $V_s = 1000$ rpm and $h = 5$ cm
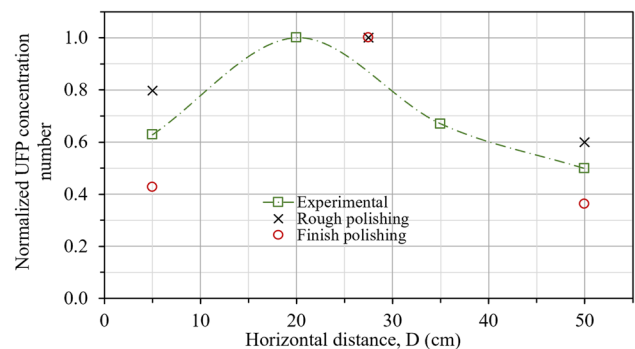

Fig. 7 Normalized UFP number concentration as a function of the horizontal distance in the experimental simulation of granite polishing phases with $V_s = 1000$ rpm
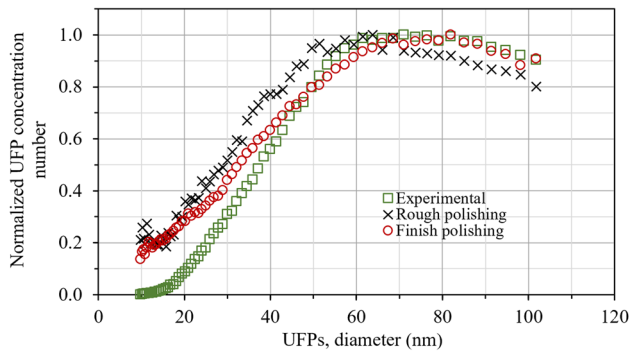
Fig. 8 UFP diameter distribution in the experimental simulation of granite polishing phases with $V_s = 1000$ rpm

Fig. 9 Efficiency of the push–pull system as a function of F_b and V_s for $F_s = 1250$ l/min

polishing process, Fig. 7). In fact, under the spindle speed effect, UFPs were ejected in horizontal direction D from the rotating disc until a peak of concentration was reached, and then this effect stopped. The maximum peak was observed for a supply flowrate of 4 l/min. After this peak, the CUFP was diluted in the air and began to decrease. For a 5 l/min supply flowrate, the peak of CUFP decreased and then the UFPs began to disperse uniformly in the horizontal direction. Therefore, from a 5 l/min supply flowrate on, the spindle speed started to have no effect on UFP dispersion. In conclusion, the supply flowrate of 4 l/min was chosen to perform the experiments for the UFP dispersion study.

Fig. 10 Efficiency of the push–pull system as a function of F_b and V_s for $F_s = 1750$ l/min

3.1.2 Dispersion Study on the Simulation Test Bench

Figure 7 shows the normalized UFP number concentration as a function of horizontal distance (D) in the experimental simulation of rough polishing and finish polishing. The spindle speed taken was 1000 rpm. The figure indicates that the UFPs dispersed (in direction D) in the same way in all three cases. The UFP concentration of NaCl and granite dust ejected from the rotating disc reached a peak at distances $D = 20$ cm and $D = 27$ cm, respectively. After this peak, the concentration started to be diluted in the air, decreasing in the horizontal direction. Figure 8 shows the UFP diameter distribution in the experimental simulation of rough polishing and finish polishing. The figure displays the same distribution shape of UFP diameters in all cases. The peaks of UFP concentration were detected for diameters close to 71, 63.8 and 82 nm, respectively, for the experimental simulation of rough polishing and finish polishing. Results in this section show that the simulation test bench effectively simulated the dispersion of granite UFPs generated during the polishing process.
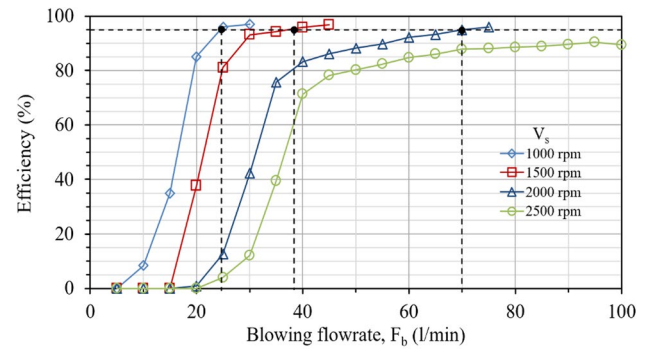

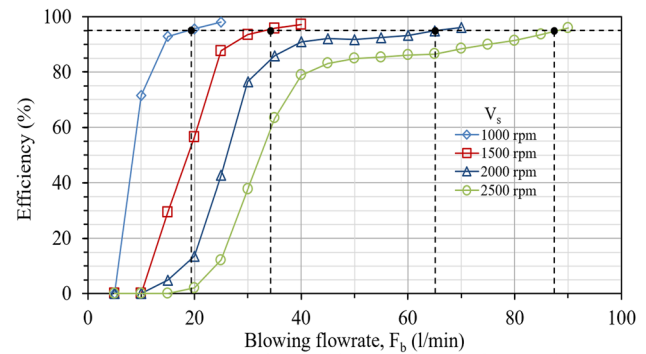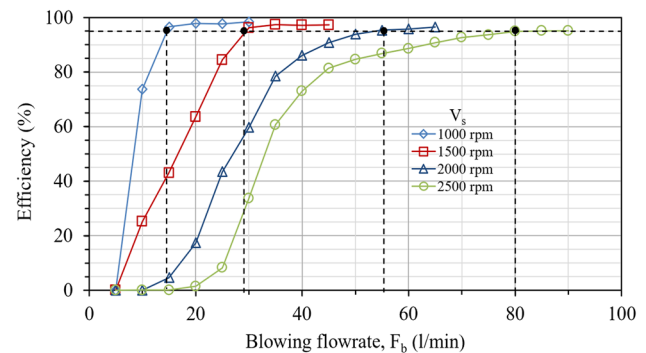**Fig. 11** Efficiency of the push–pull system as a function of F_b and V_s for $F_s = 2250$ l/min

3.2 Evaluation of the LEV System's Efficiency

This part of the study evaluated the efficiency of three LEV systems (push–pull, dust shroud and integrated suction slots) designed to capture UFPs generated during the polishing process.

3.2.1 The Push–Pull System

Figures 9, 10 and 11 show the 95% efficiency of the push–pull system as a function of the blowing flowrate (from the blowing holes) and spindle speed (of the rotating disc) for, respectively, 1250, 1750 and 2250 l/min suction flowrates (of the exhaust hood). These figures show that when the spindle speed increased, the blowing flowrate needed to direct UFPs to the exhaust hood also increased. In fact, raising the spindle speed increased the velocity of the emitted UFPs. Consequently, it was necessary to augment the blowing flowrate to overcome the strongest UFP motion. The figures also show that increasing the suction flowrate of the exhaust hood decreased the blowing flowrate. In fact, the negative pressure generated by the exhaust hood increased with the suction flowrate, resulting in the UFPs moving faster to the exhaust hood. This, in turn, reduced the blowing flowrate needed to direct the UFPs to the exhaust hood. For the suction flowrate of 1250 l/min, it was impossible to find the blowing flowrate needed to transport UFPs to the exhaust hood for the spindle speed of 2500 rpm. In fact, large numbers of UFPs reached the exhaust hood but remained outside because the suction of 1250 l/min was insufficient to evacuate them all.

Figure 12 shows the blowing flowrate needed to direct the UFPs to the exhaust hood as a function of the spindle speed and suction flowrate. It also shows that there was a linear relationship between the blowing flowrate F_b and the spindle speed V_s. This relationship is expressed for each suction flowrate as follows:

$$F_b = 0.05 V_s - f(F_s), \tag{2}$$

where $f(F_s)$ is the constant of Eq. (2), depending on the suction flowrate and is determined in Fig. 13 as follows:
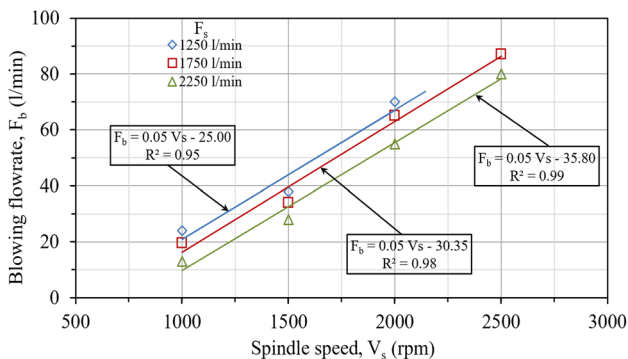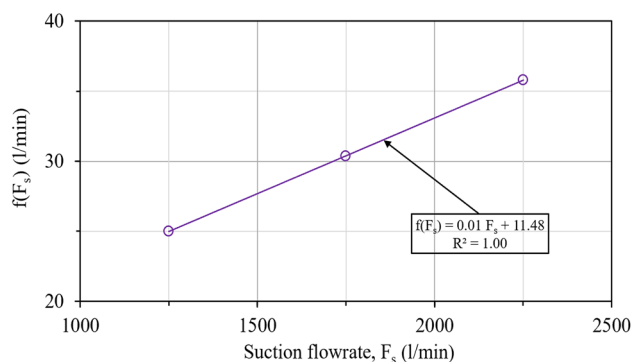
$$f(F_s) = 0.01 F_s + 11.48. \tag{3}$$

Fig. 13 Determination of $f(F_s)$ function

Replacing Eq. (3) with Eq. (2) gives the final relationship between F_b, V_s and F_s. Eq. (4) expresses the final relationship:

$$F_b = 0.05 V_s - 0.01 F_s - 11.48. \tag{4}$$

This relationship between F_b, V_s and F_s was valid for the spindle speed interval [1000, 2500] rpm. In addition, this relationship helped configure the push–pull system for any given situation.

3.2.2 The Dust Shroud

Figure 14 shows the 95% efficiency of the dust shroud as a function of suction flowrate and spindle speed. The figure indicates that for spindle speeds varying from 1000 to 2500 rpm, a suction flowrate of 14 l/min was sufficient to evacuate 95% of the UFPs ejected by the rotating disc. The UFP supply flowrate was thus constant; the suction flowrate needed to evacuate the UFPs had to be constant even if the spindle speed changed. With the suction flowrate of 15 l/min, the dust shroud system ensured 100% evacuation of the UFPs emitted by the rotating disc.
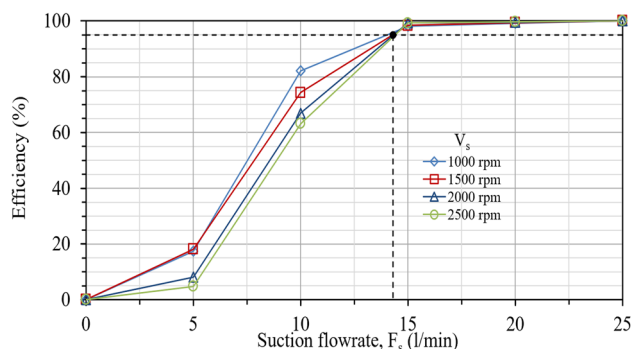

Fig. 12 Blowing flowrate (F_b) as a function of spindle speed (V_s) and suction flowrate (F_s)

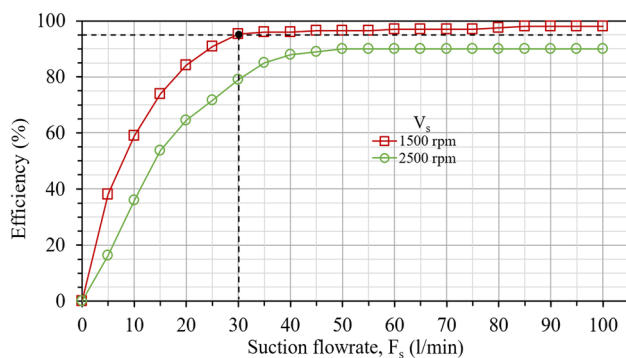**Fig. 14** Efficiency of the dust shroud as a function of suction flowrate and spindle speed

Fig. 15 Efficiency of the tool with integrated suction slots as a function of suction flowrate and spindle speed

3.2.3 The Tool with Integrated Suction Slots

Figure 15 shows the 95% efficiency of the tool with integrated suction slots as a function of suction flowrate and spindle speed. For a low spindle speed of 1500 rpm, the suction flowrate needed to evacuate UFPs (ejected by the rotating disc) through the suction slots was 30 l/min. For a high spindle speed of 2500 rpm, the suction flowrate needed to ensure 95% efficiency of UFP evacuation could not be reached. For a high spindle speed, the UFPs ejected with high velocity could not be effectively captured with the current suction slots. It is recommended that slots be added on the lateral side of the rotating disc to increase the suction velocity. Increasing the suction velocity should facilitate the capture of the UFPs ejected by the rotating disc.

4 Conclusion

This study (1) validated that the experimental test bench indeed simulated the dispersion of UFPs generated during the polishing process, and (2) studied the efficiency of three LEV systems in reducing the UFPs released by this process.

The calibration of the UFP supply flowrate on the simulation test bench showed that a flowrate of 4 l/min was sufficient to simulate UFP dust dispersion during the polishing process. The results obtained in the test bench for UFP dispersion and their diameter distribution were similar to those in the polishing process of granite. In fact, the CUFP over horizontal distance (D) reached a peak and then decreased, in all cases. Also, the UFP diameter distribution had the same shape for both the experimental test bench and the actual polishing process. The experimental simulation is, therefore, considered appropriate for simulating UFP dispersion in the granite polishing process.

The validated experimental simulation bench was used to study the efficiency of three LEV systems in reducing the quantity of UFPs generated during the granite polishing process. The study of the push–pull system showed a relationship between the blowing flowrate, spindle speed and suction flowrate. This relationship helped configure this LEV system for spindle speeds from 1000 to 2500 rpm. The results of the push–pull system investigation showed that this approach can be used to tackle other sources of UFP emissions, such as processes used in the chemical industry. The study of the dust shroud revealed that using a suction flowrate of 14 l/min was sufficient to evacuate UFPs for spindle speeds ranging from 1000 to 2500 rpm. The study of the tool with integrated suction slots showed that the present design was efficient for low spindle speeds. For high spindle speeds, lateral side slots would need to be added to improve the velocity of UFP capture.

The efficiency of the three LEV systems was very sensitive to suction flowrate and spindle speed. Consequently, it is difficult to accurately predict dust removal in industrial environments, where particular and varying configurations are found. The three LEV systems were shown to have more than 95% efficiency. Despite this result, it is believed that LEV systems still require on-site adjustment during industrial polishing processes. To further reduce UFP concentrations, these systems could be combined, but this would imply a higher cost.

References

ACGIH (2010) Industrial ventilation: a manual of recommended practice for design, 27th edn. American Conference of Governmental Industrial Hygienists, Cincinnati

Ahmad I, Khan MI, Patil G (2011) Nanotoxicity of occupational dust generated in granite stone saw mill. In: 2011 International Conference on nanoscience, technology and societal implications, pp 1–6. https://doi.org/10.1109/nstsi.2011.6111990

Akbar-Khanzadeh F, Milz S, Ames A, Susi PP, Bisesi M, Khuder SA, Akbar-Khanzadeh M (2007) Crystalline silica dust and respirable particulate matter during indoor concrete grinding—wet grinding and ventilated grinding compared with uncontrolled conventional grinding. J Occup Environ Hyg 4:770–779. https://doi.org/10.1080/15459620701569708

Bahloul A, Djebara A, Saidi MN, Songmene V, Villalpando F, Reggio M (2019) Computational and experimental analysis of ultrafine particle dispersion during granite polishing. Aerosol Sci Eng 3:21–31. https://doi.org/10.1007/s41810-018-00038-7

Croteau GA, Guffey SE, Flanagan ME, Seixas NS (2002) The effect of local exhaust ventilation controls on dust exposures during concrete cutting and grinding activities. AIHA J 63:458–467

Fanizza C et al (2007) Cytotoxicity and DNA-damage in human lung epithelial cells exposed to respirable α-quartz. Toxicol In Vitro 21:586–594. https://doi.org/10.1016/j.tiv.2006.12.002

Goyer N, Bahloul A, Veillette C (2010) Prévention de l'exposition des travailleurs à la silice. Institut de recherche Robert-Sauvé en santé et en sécurité du travail (IRSST), Québec

ICRP (1994) Human respiratory tract model for radiological protection. ICRP Publication 66. Ann. ICRP 24 (1-3). https://www.coursehero.com/file/43423254/ICRP-66-The-Human-Respiratory-Tract-Model-Ann-ICRP-241-3-1994pdf/

Johnson DL, Phillips ML, Qi C, Van AT, Hawley DA (2017) Experimental evaluation of respirable dust and crystalline silica controls during simulated performance of stone countertop fabrication tasks with powered hand tools. Ann Work Expo Health 61:711–723. https://doi.org/10.1093/annweh/wxx040

Kusaka T, Nakayama M, Nakamura K, Ishimiya M, Furusawa E, Ogasawara K (2014) Effect of silica particle size on macrophage inflammatory responses. PLoS One 9:e92634. https://doi.org/10.1371/journal.pone.0092634

Li Y, Huang H, Xu XP (2006) Gloss formation and its relationship with roughness in granite grinding. Key Eng Mater 304–305:413–416

Liu Y et al (2013) Exposure-response analysis and risk assessment for lung cancer in relationship to silica exposure: a 44-year cohort study of 34,018 workers. Am J Epidemiol 178:1424–1433. https://doi.org/10.1093/aje/kwt139

Martínez C, Prieto A, García L, Quero A, González S, Casan P (2010) Silicosis: a disease with an active present. Arch Bronconeumol (English Edition) 46:97–100. https://doi.org/10.1016/S1579-2129(10)70022-7

McDonald JC, McDonald AD, Hughes JM, Rando RJ, Weill H (2005) Mortality from lung and kidney disease in a cohort of North American industrial sand workers: an update. Ann Occup Hyg 49:367–373. https://doi.org/10.1093/annhyg/mei001

OSHA (2019) Silica, crystalline, mixed respirable (quartz, cristobalite, tridymite). Occupational Safety and Health Administration, U.S. Department of Labor. https://www.osha.gov/chemicaldata/chemResult.html?RecNo=278. Accessed 6 May 2019

Pelucchi C, Pira E, Piolatto G, Coggiola M, Carta P, La Vecchia C (2006) Occupational silica exposure and lung cancer risk: a review of epidemiological studies 1996–2005. Ann Oncol 17:1039–1050. https://doi.org/10.1093/annonc/mdj125

Phillips ML, Johnson DL, Johnson AC (2013) Determinants of respirable silica exposure in stone countertop fabrication: a preliminary study. J Occup Environ Hyg 10:368–373

ROHS (2019) Regulation respecting occupational health and safety. Légis Québec. http://legisquebec.gouv.qc.ca/fr/showdoc/cr/S-2.1,%20r.%2013. Accessed 14 Jan 2019

Rushton L (2007) Chronic obstructive pulmonary disease and occupational exposure to silica. Rev Environ Health 22:255. https://doi.org/10.1515/reveh.2007.22.4.255

Saidi MN, Songmene V, Kouam J, Bahloul A (2015) Experimental investigation on fine particle emission during granite polishing process. Int J Adv Manuf Technol 81:2109–2121

Saidi MN, Songmene V, Kouam J, Bahloul A (2018) Rotational and translation-free polishing of granite: surface quality and dust particles emission and dispersion. Int J Adv Manuf Technol 98:289–303. https://doi.org/10.1007/s00170-018-2247-8

Silverman L, Billings CE (1956) Methods of generating solid aerosols. Air Pollut Control Assoc J 6:76–83

Simcox NJ, Lofgren D, Leons J, Camp J (1999) Silica exposure during granite countertop fabrication. Appl Occup Environ Hyg 14:577–582

Songmene V, Kouam J, Balhoul A (2018) Effect of minimum quantity lubrication (MQL) on fine and ultrafine particle emission and distribution during polishing of granite. Measurement 114:398–408. https://doi.org/10.1016/j.measurement.2017.10.012

Steenland K, Ward E (2014) Silica: a lung carcinogen. CA Cancer J Clin 64:63–69

Verma DK, Vacek PM, des Tombe K, Finkelstein M, Branch B, Gibbs GW, Graham WG (2011) Silica exposure assessment in a mortality study of Vermont granite workers. J Occup Environ Hyg 8:71–79

Wang Y, Zou Y, Yang Y, Wu S, Zhang X, Ren X (2016) Movement and control of evaporating droplets released from an open surface tank in the push–pull ventilation system. Build Simul 9:443–457. https://doi.org/10.1007/s12273-016-0276-5

Xu XP, Huang H, Li Y (2003) Material removal mechanisms in diamond grinding of granite, Part 1: the morphological changes of granite from sawing to grinding. Key Eng Mater 250:215–221

Yaonan C, Li L, Haiting W, Mingyang W, Yizhi L (2014) Investigations on the dust distribution characteristics of dry milling using inserts with various groove profiles. Int J Adv Manuf Technol 74:551–562. https://doi.org/10.1007/s00170-014-6019-9

Yavuz H, Ozkahraman T, Demirdag S (2011) Polishing experiments on surface quality of building stone tiles. Constr Build Mater 25:1707–1711. https://doi.org/10.1016/j.conbuildmat.2010.10.016

Zhang Z, Kleinstreuer C, Donohue JF, Kim CS (2005) Comparison of micro- and nano-size particle depositions in a human upper airway model. J Aerosol Sci 36:211–233. https://doi.org/10.1016/j.jaerosci.2004.08.006